Shape of Complexity

Manuel Reta[1], Konstantin Holzhausen[2], and Knut Erik Knutsen[3]

[1,2,3] *Data Driven Services, Maritime Group Research and Development, DNV, Veritasveien, 1322 Høvik, Norway*
Manuel.Guillermo.Reta@dnv.com
Konstantin.Holzhausen@dnv.com
Knut.Erik.Knutsen@dnv.com

ABSTRACT

Failure in complex engineered systems does not occur, as a simple or linear accumulation of independent component faults. Their failure modes are often relational: degradation propagates through feedback loops, coupling pathways, and many-body interactions among sensors, controllers, and actuators. This creates a gap for prognostics and health management, where many established approaches still interpret system health primarily through single-channel indicators or pairwise summaries.

This paper argues for a broader PHM perspective in which system health is read from the structure of interactions rather than from isolated signals alone. Simplicial complexes provide a natural representation for this purpose because they encode both pairwise and higher-order relations, while topological descriptors such as Betti numbers compress that relational structure into interpretable, threshold-robust signatures.

Within this perspective, we use an interconnectivity pipeline based on mutual information, temporal lag, coupling modality, and O-information as one concrete example of how multichannel data can be converted into a simplicial complex and analysed topologically. We validate and tune our method using an analytic toy model in which connectivity between components can be controlled. As part of this, we discuss what different interaction measures can and can not recover. A double-loop controller motor experiment then illustrates the PHM value of the approach: edge density, mean edge strength, and persistent loop structure vary systematically across fault conditions even when no single signal provides an equally clear separation. Together these results provide evidence that relational and topological descriptions can extend PHM beyond the single-signal view of system health.

1. INTRODUCTION

Modern engineered systems are characterised by dense functional coupling: sensors, controllers, and actuators interact across multiple timescales and frequency ranges, and it is precisely this integration that enables advanced functionality and high adaptability through emergence. The same integration, however, means that failure modes are rarely localised. Cascading failures, feedback-driven degradation, and emergent collapse are phenomena in which a fault in one component alters the operating regime of others, which in turn modifies loading on a third, until a system-wide event occurs that could not have been predicted from any single signal (Battiston et al., 2020).

Traditional prognostics and health management (PHM) addresses this challenge predominantly through single component condition monitoring: one model per sensor, one threshold per indicator. This strategy is inherently additive, it treats observed complexity as the linear sum of independent component risks. It misses the relational structure of the system: the fact that health or degradation is encoded not only in signal amplitudes but in *how signals interact*, how they synchronise, lead one another in time, and form functional units. A controller and the motor it drives may individually appear within specification while their mutual coupling has already degraded to the point of imminent failure.

To monitor the relational structure of a system one needs a representation in which interaction is a first-class object. Graphs provide one such representation, but they capture only pairwise relations; engineered feedback loops and redundant sensor arrays are inherently multi-body structures (Torres, Blevins, Bassett, & Eliassi-Rad, 2021). Several families of methods already move in this direction: correlation and coherence networks, information-theoretic connectivity measures, graph-based monitoring, and more recent higher-order network constructions. Each captures part of the problem, but often with limitations in handling nonlinearity, temporal offset, cross-frequency structure, or higher-order functional organisation. The aim of this paper is not to argue for a single definitive

replacement, but to motivate a broader PHM viewpoint in which system health is inferred from the organisation of interactions. Within that viewpoint, we use informational entropy metrics, together with our interconnectivity pipeline, as a concrete worked example.

The paper therefore proceeds as follows:

1. Demonstration of simplicial complexes as a representation for complex system health beyond pairwise graphs. (Section 2);
2. Reviews how interaction measures can be lifted into constructing hypernetworks, and positions our interconnectivity method as one example among several possible routes. (Section 3);
3. Shows how topological summaries such as Betti numbers and Hodge-type decompositions make the resulting structure interpretable for PHM (Section 4); and
4. Validates and illustrates the idea with a double-looped motor controller simulation experiment (Sections 5–6).

2. COMPLEX SYSTEMS AND SIMPLICIAL COMPLEXES

A graph captures pairwise relationships between system components: edges connect pairs of nodes, and any group interaction must be decomposed into dyads. For many engineered systems this is insufficient. A feedback control loop couples sensor, controller, and actuator jointly: removing any one breaks the functional circuit, and the loop's failure mode differs qualitatively from the failure of any pair within it. Representing this structure requires a formalism in which higher-order interactions are native objects, not derived approximations.

A simplicial complex: $\mathcal{K}$ is a collection of simplices, vertices (0-simplices), edges (1-simplices), triangles (2-simplices), and higher-dimensional analogues which satisfy the face axiom: if $\sigma \in \mathcal{K}$ then every face of σ is also in $\mathcal{K}$ (Torres et al., 2021). In our framework each system component (sensor output, actuator signal, controller variable) corresponds to a vertex; each validated pairwise functional coupling to an edge; and each three-way interaction to a triangle (2-simplex). The complex therefore encodes the multi-body interaction architecture of the system as a whole, in a mathematically rigorous object that supports both combinatorial (graph-theoretic) and continuous (topological) analysis.

Edges carry a normalised information-theoretic distance $d_{ij} \in [0,1]$. Values near zero indicate strong coupling; values near one indicate statistical independence. This distance representation means the edge-weight matrix serves directly as a dissimilarity matrix for downstream TDA without further transformation. Triangles are annotated with the O-information (Rosas, Mediano, Gastpar, & Jensen, 2019) of their constituent triple, which classifies functional groups as *redundant* ($\Omega > 0$: two members share overlapping information about the third, characteristic of sensor redundancy and common-driver configurations) or *synergistic* ($\Omega < 0$: emergent information only accessible when all three are observed jointly, characteristic of tight closed-loop circuits). Both signatures carry diagnostic relevance: the degradation of a synergistic triplet towards redundancy, or the disappearance of a triangle altogether, indicates loss of functional coupling within that component group.

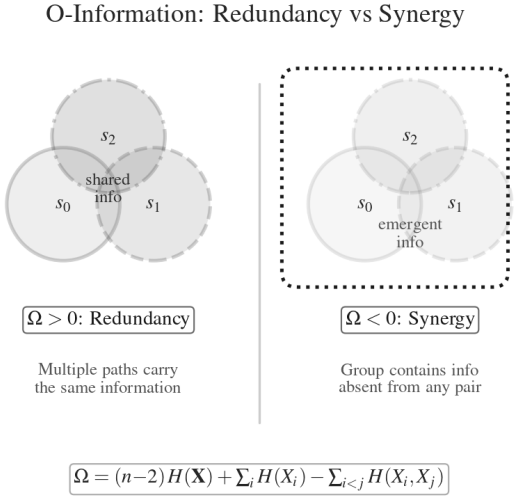

Figure 1. O-information decomposition over an example triplet of system components. Positive Ω (redundancy) indicates a shared driver or backup-sensor configuration; negative Ω (synergy) indicates a tight joint dependency characteristic of a closed feedback loop.

3. METHODOLOGY: FROM INTERACTION MEASURES TO FUNCTIONAL TOPOLOGY

There is no single mandated way to map multichannel engineering data into a relational system model. Depending on the target physics and data regime, one may use correlation, coherence, transfer entropy, distance correlation, HSIC (Herbert Schmidt independence criteria), mutual information, or hybrid physics-informed measures to define interactions. Likewise, higher-order structure may be introduced through clique expansion, hypergraphs, simplicial complexes, or motif-based summaries.

In this paper we use our interconnectivity pipeline as one concrete example of how such a mapping can be performed. Connectivity becomes a multidimensional, multipronged approach here because it combines nonlinear dependence, temporal lag, coupling modality, and higher-order annotation in a single construction. However, the broader argument of the paper does not depend on this exact choice. The purpose of this section is therefore illustrative: to show one plausible route from multichannel signals to a relational system model that can then be interpreted topologically. The pipeline maps

a multichannel matrix $\mathbf{X} \in \mathbb{R}^{N \times C}$ (N samples, C channels) into a weighted simplicial complex through four stages: decomposition, encoding, edge construction, and higher-order annotation.

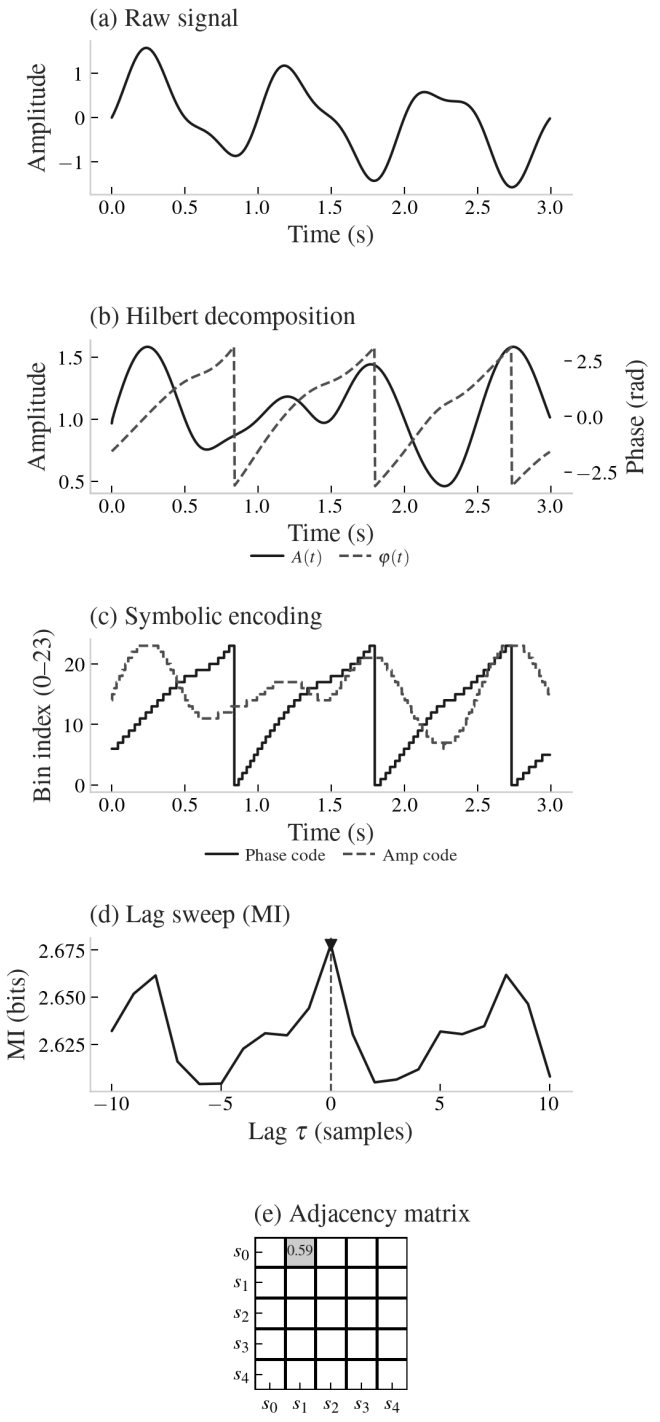

Figure 2. Methodology pipeline: from raw multichannel time series to functional simplicial complex and topological health signatures.

3.1. Signal Decomposition and Encoding

Each channel $x_c(t)$ is processed via the analytic signal to yield instantaneous amplitude and phase:

$$z_c(t) = x_c(t) + i\,\mathcal{H}[x_c(t)], \quad A_c(t) = |z_c(t)|, \quad \varphi_c(t) = \arg(z_c(t)), \tag{1}$$

where $\mathcal{H}[\cdot]$ denotes the Hilbert transform (Picinbono, 1997). Channels whose instantaneous frequency variance exceeds a configurable threshold are flagged as lacking reliable phase estimates and excluded from phase-dependent coupling modalities; they remain available for amplitude–amplitude analysis.

Encoding converts continuous components to discrete symbol sequences. Phase is mapped to B equidistant sectors on $[-\pi, \pi]$ via linear binning, which yields a near-uniform distribution for a free-running oscillator and preserves synchronisation structure as consistent bin offsets. Amplitude is discretised with bins anchored at zero ($\lfloor B \cdot A(t)/A_{\max} \rfloor$), ensuring that a constant-amplitude signal occupies a single bin (entropy ≈ 0) rather than inflating numerical noise into apparent modulation. Ordinal-pattern encoding, while useful for raw time-series complexity analysis, is inappropriate for phase: because phase is locally monotonic, ordinal patterns collapse to near-constant sequences, destroying synchronisation information entirely.

3.2. Edge Construction: Strength, Lag, and Modality

For each channel pair (i, j) the example pipeline computes mutual information

$$I(X;Y) = H(X) + H(Y) - H(X,Y) \tag{2}$$

across three coupling modalities: *phase–phase* (PP) captures frequency synchronisation, *amplitude–amplitude* (AA) captures co-modulation of envelopes, and *phase–amplitude* (PAC) captures cross-frequency coupling in which the phase of one channel modulates the amplitude of another (Canolty & Knight, 2010).

Coupling is evaluated at a sweep of temporal lags: $\ell \in \{-L_{\max}, \ldots, +L_{\max}\}$:

$$I^*_{ij} = \max_{\ell}\, I(X_i(t),\, X_j(t+\ell))\,. \tag{3}$$

Each edge therefore carries three co-registered quantities: (1) coupling *strength* as a normalised distance:

$$d_{ij} = 1 - I^*/D_{\text{mode}} \in [0,1] \tag{4}$$

the preferred *time lag* ℓ^* indicating the direction of temporal precedence, and (3) the dominant coupling *modality*. This is richer than scalar correlation: an edge between a motor current sensor and a position encoder may show AA coupling at a lag of several hundred milliseconds, directly recovering the electromechanical propagation delay and distinguishing it

from zero-lag phase synchronisation.

Other interaction measures could be substituted at this stage. Correlation-based edges would emphasise linear co-variation, transfer entropy would prioritise directional predictability, and kernel-based dependence measures could capture nonlinear relations without discretisation. The point is not that mutual information is universally optimal, but that a PHM pipeline should make its relational assumptions explicit and then carry them consistently into the topological representation.

The modality-specific normalisation denominator D_{mode} corresponds to the theoretical maximum MI of the relevant encoding (Tort, Komorowski, Eichenbaum, & Kopell, 2010), bounding d_{ij} within $[0, 1]$ regardless of encoding resolution, so that distances are comparable across modalities. Edge significance is assessed via surrogate shuffle testing and Benjamini - Hochberg FDR correction (Theiler et al., 1992; Benjamini & Hochberg, 2018); non-significant edges are removed and their distance set to 1.

3.3. Higher-Order Annotation: O-Information

There are different ways to capture higher-order information exchange between more than two components. Rosas et al. generalizes Mutual Information to triplets of constituents. Their metric O-Information measures whether knowing the joint triplet of constituent states in addition the lower order states captures more information about the system then knowledge about the pairs and singlets alone. For every clique of size 3 in the thresholded graph, the O-information is computed over the encoded streams of the three member channels (Rosas et al., 2019):

$$\Omega(X_1; X_2; X_3) = \sum_{i=1}^{3} H(X_i) - H(X_1, X_2, X_3) - \sum_{i<j} I(X_i; X_j) \tag{5}$$

Each significant triplet is promoted to a 2-simplex in $\mathcal{K}$, annotated with its Ω value and redundancy/synergy classification. In summary, Mutual Information and O-Information together capture interactions between pairs and triplets of components, forming a clique-complex representation up to cliques of size 3.

Alternatively, one can encode dyadic relations in distances by Equation 4. This approach transforms the problem into connectivity analysis on a point cloud defined by those distances between signals, for which a variety of methods exists. Next to the distance metric in Equation 4, which is based on the Geometric Normalized Mutual Information with $D_m = \sqrt{H(X_1) \cdot H(X_2)}$, we have also studied point clouds on the basis of distance correlation and Pearson distance. Choosing any distance value as a threshold for connectivity defines the Vietoris-Rips simplicial complex on the network of connections that survive. In this context, the threshold distance value is called the scale ϵ of the Vietoris-Rips complex. What is left to do is to select the right scale at which the features of interest are present. Computational persistent cohomology analysis, a method from topological data analysis offers a way to detect if interesting connectivity shapes are present.

4. CONNECTIVITY AND TOPOLOGY

The edge distance matrix $\mathbf{D}$ produced by the pipeline is a symmetric dissimilarity matrix with $d_{ij} \in [0, 1]$, inducing a point cloud where every pair of points (i, j) is separated by distance d_{ij}. This deliberate choice, using distance rather than similarity as the edge representation, connects the functional network construction to the filtration-based methods of numerical algebraic topology.

4.1. Vietoris–Rips Filtration and Persistent Cohomology

A *Vietoris–Rips complex* $\mathcal{VR}_\epsilon(\mathbf{D})$ is formed by inserting a k-simplex whenever all pairwise distances among its $k + 1$ vertices fall below threshold ϵ. Variation of this scale parameter ϵ induces a nested sequence of Vietoris-Rips complexes. Topological features are captured by persistent features read from persistence diagrams.

- $\mathbf{H}_0$: connected components
- $\mathbf{H}_1$: independent loops: persistent loops correspond to 1-dimensional functional cycles in the network — e.g., the closed-loop control path sensor $\rightarrow$ controller $\rightarrow$ actuator $\rightarrow$ plant $\rightarrow$ sensor — that cannot be "filled" by triangles. Their disappearance or shortening indicates loss of cyclic functional coupling.
- $\mathbf{H}_2$ (2D voids): higher order features, for example caused by interactions involving functional cycles

Because the Vietoris-Rips construction includes the filled simplex whenever all pairwise distances fall within ϵ, any three mutually close constituents form a filled triangle, immediately closing the corresponding 1-cycle. Persistent H_1 features therefore correspond only to loops formed by four or more constituents.

4.2. Hodge Laplacian Spectrum

The Hodge Laplacian $\mathbf{L}_i = \mathbf{B}_i^\top \mathbf{B}_i + \mathbf{B}_{i+1}\mathbf{B}_{i+1}^\top$ generalises the graph Laplacian $\mathbf{L}$ to simplicial complexes on graphs, where $\mathbf{B}_i$ and $\mathbf{B}_{i+1}$ are the boundary operators mapping between the spaces of i- and $i + 1$-simplices. Because we are interested in 1-cycles, we work with L_1 whose boundary matrices map edges to vertices and triangles to edges, respectively.

The kernel $\ker L_1$ consists of harmonic cycles, edge flows with no source or sink, which identify closed functional loops in the network. The non-zero spectrum decomposes into gradient flows (localised information sources, node-driven) and curl flows (local circulating interactions, triangle-driven), pro-

viding a spectral decomposition of the system's interaction topology. Crucially, zero eigenvectors of $\mathbf{L}_1$ provide unique minimum-norm representatives of each topologically independent cycles, allowing individual components to be identified as structural participants in specific loop or flow features. Overall, the spectrum of the Hodge Laplacian encodes a variety of structural information that provides effective representations for both system characterization and anomaly detection (Frantzen & Schaub, 2025).

5. VALIDATION I: RING OF ORNSTEIN-UHLENBECK PROCESSES

To validate our topological method, we chose a toy model of a set of N identitical Ornstein-Uhlenbeck processes that are connected in a ring structure. The dynamics of each processes x_i are described by an Itô Stochastic Differential Equation with leak current proportional to α and upstream neighbor coupling with coupling strength $\frac{1}{\tau}$.

$$dx_i = \left(-\alpha x_i + \frac{x_{i-1 \bmod N} - x_i}{\tau}\right) dt + \sigma\, dW_i \qquad (6)$$

The system's circular connectivity induces a directed clockwise signal cascade $\ldots x_i \to x_{i+1 \bmod N} \to \ldots$ corresponding to one topologically independent 1-cycle in the simplicial complex. As a result, we expect a clear H_1 signal in the persistence diagrams. Figure 3 shows H_1 persistence for the ring system both as a function of effective coupling strength between neighboring processes and number of constituents n. Because the choice of connectivity measure is arbitrary, we tested persistence with regard to three different distance metrics capturing the degree of interaction at different levels of complexities. The Pearson correlation distance d_P only captures linear correlations between signals, whereas the distance correlation d_{dCorr} also accounts for potential non-linear relations. The information-theoretic Normalized Mutual Information distance d_{NMI} is able to capture arbitrarily complex statistical dependencies between signals and is, therefore, considered the most advanced. It is apparent, that strongly interacting systems are characterized by short persistences which result in weak H_1 signals. As a result, cycles in these systems might not be resolved by advanced metrics but only weaker, correlation-based ones. In summary, the level of structural topological features that can be extracted also depends on the metric the analysis is based on.

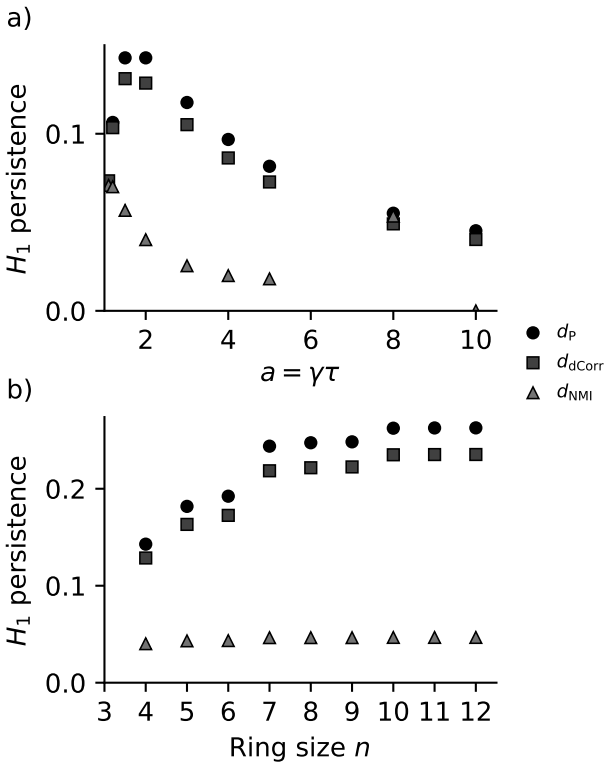

Figure 3. H_1 persistence as a function of effective coupling strength $a \propto \alpha\tau$ and number of processes n for three different connectivity measures: Pearson-correlation distance d_P, distance correlation d_{dCorr}, and Normalized Mutual Information distance d_{NMI}. **a)**: The stronger the interaction, the less persistent the topological feature. There is a clear order between the measures as well. The more statistical information the measure picks up, the weaker the feature signal appears with strong interactions. **b)**: Persistence as a function of ring size. The bigger the ring, the more persistent the feature. The effect is more pronounced with weaker measures. d_{NMI} shows almost no sensitivity to n compared to the other metrics.

6. VALIDATION II: DOUBLE-CONTROLLER MOTOR EXPERIMENT

The broader PHM argument is illustrated on a motor controller dataset with a double-controller architecture, where multichannel interactions are expected to carry more information than any one sensor stream in isolation. The example comprises time-series recordings under conditions defined by three binary factors: motor health (nominal vs. faulty), drive signal type (constant vs. oscillating input), and motor age (new vs. old). The new vs old motor age was simulated by increased noise in the signal. The full factorial design yields eight operating conditions, providing a structured test of which network-level quantities carry fault information. This case is intentionally more realistic than the ring benchmark because the diagnostic question is no longer "is the topology recovered exactly?" but "does a relational description expose health differences that the single-signal view suppresses?" Because the setup contains interacting controller pathways rather than a single idealised loop, it also provides a better bridge to the kind of coupled subsystem behaviour PHM encounters in practice.

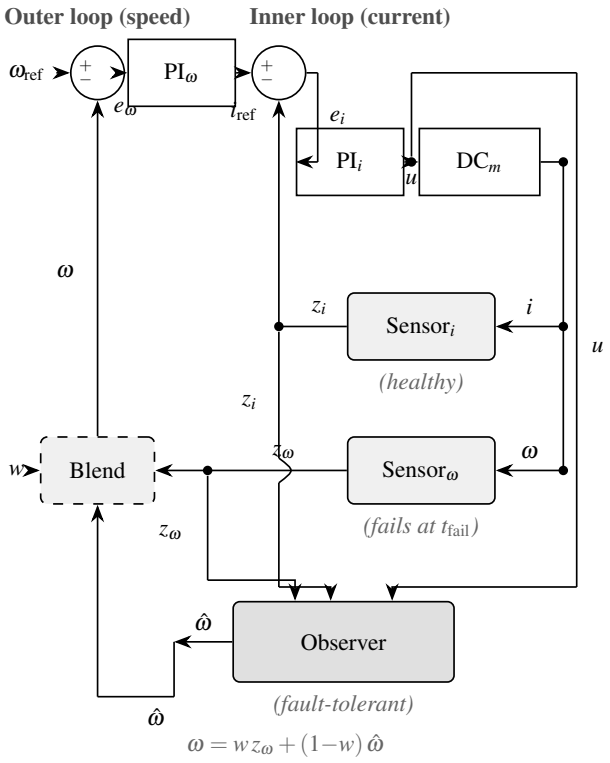

Figure 4. Double loop controller schematic

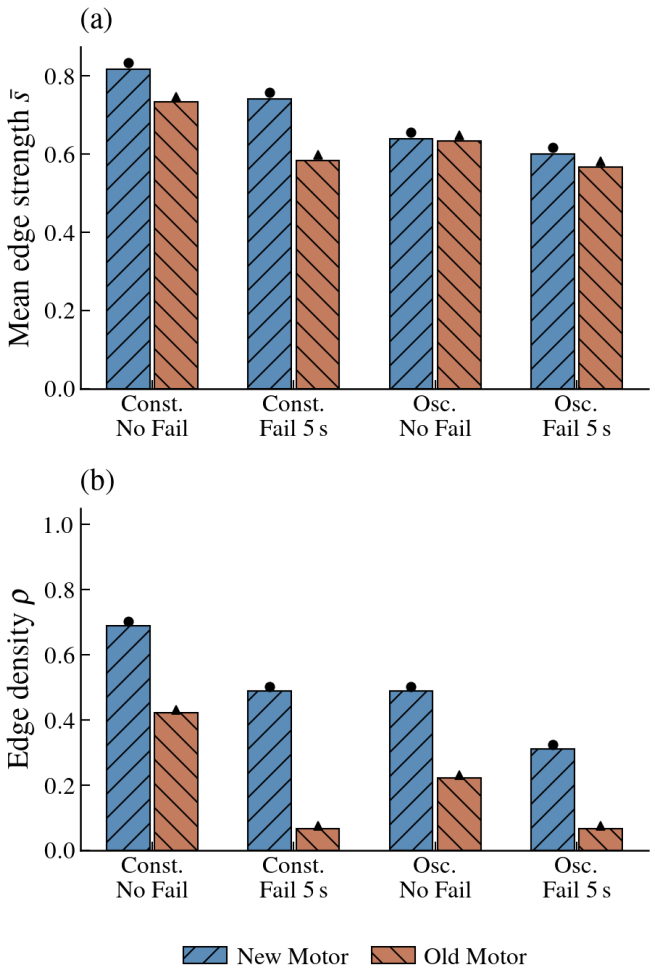

Figure 5. Edge density (left) and mean edge strength (right) of the functional network across fault conditions. Faulty operation is characterised by significantly reduced connectivity and weaker mean coupling — signatures that are not recoverable from any individual signal channel.

6.1. Network Metrics Across Conditions

Figure 5 shows edge density and mean edge strength across the experimental conditions. Two results stand out. First, the fault condition produces a marked reduction in both metrics: the faulty system has fewer and weaker functional connections, consistent with the physical interpretation that motor degradation decouples the functional architecture of the double-controller system. Second, oscillating input yields higher edge density than constant input — the richer excitation better reveals the latent coupling structure of the system, a practical consideration for active health monitoring strategies (scheduled oscillatory tests may provide more diagnostic information than constant-setpoint operation).

These findings have a direct PHM interpretation: edge density integrates information across all channels simultaneously. No individual signal shows the clear separation between conditions visible in the network metric. The diagnostic information is genuinely distributed across the relational structure of the system, not localised in any single sensor, precisely the scenario for which component based condition monitoring is insufficient.

6.2. Topological Health Signatures

Topological data analysis applied to the functional distance matrix reveals that the healthy nominal condition consistently sustains a significant H_1 feature — a loop in the connectivity structure corresponding to the dominant closed-loop pathway across the double-controller architecture. Under faulty operation this feature weakens or disappears: degradation breaks the functional cycle and the feedback loop ceases to manifest as a topological hole in the simplicial complex. The topological signature is threshold-independent: it persists across the entire filtration range, making it a robust health indicator that does not require manual tuning of a coupling cutoff.

Together, the two results — a network metric (edge density) and a topological invariant (H_1 persistence) — provide complementary views of the same physical event: the metric captures that "something changed in the network", while the topo-

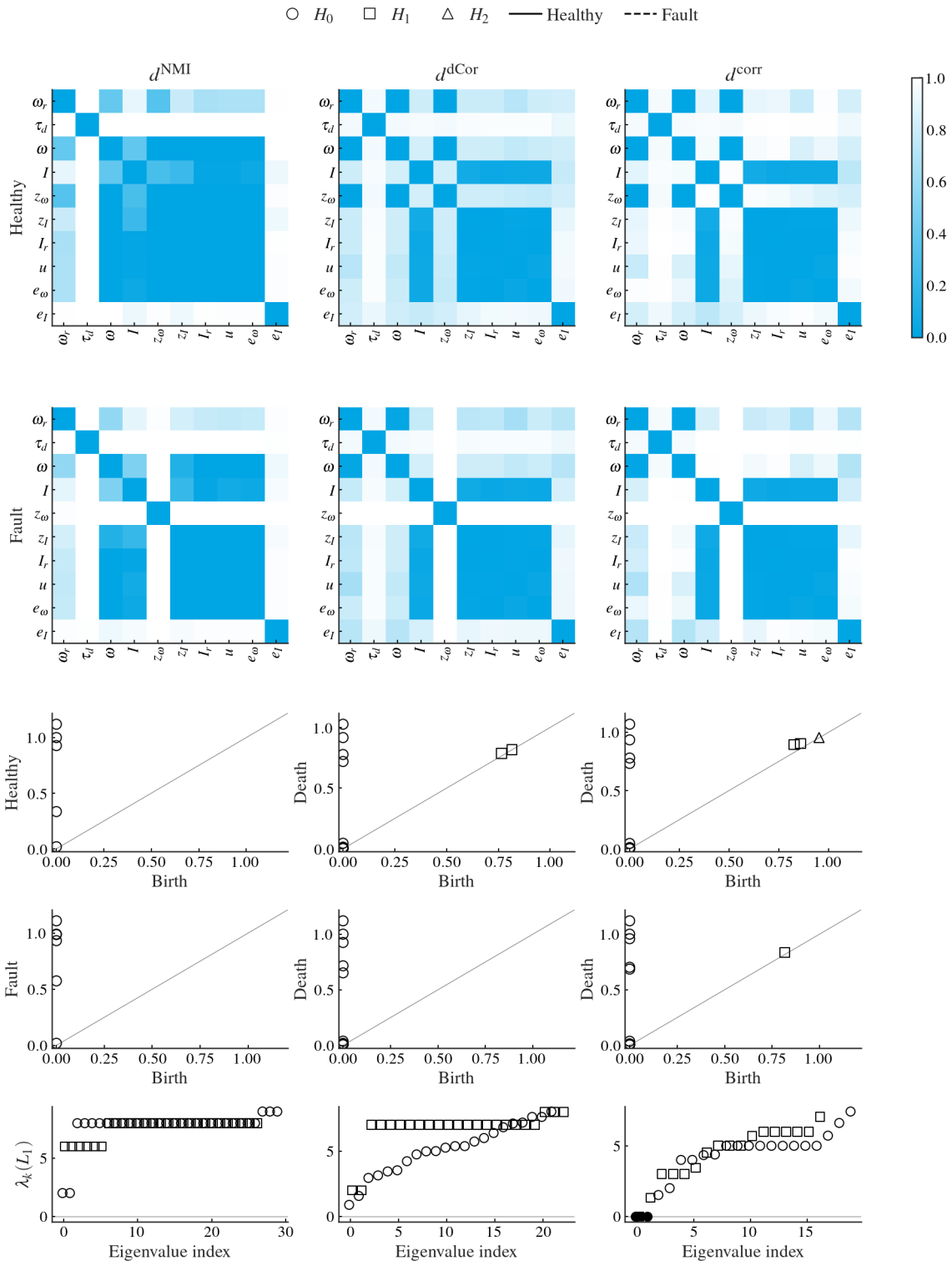

Figure 6. Comparison of information flow topologies induced by different metrics between a flawlessly operating cascading control cycle and one operating in the fail-safe state due to a broken angular velocity sensor. Non-trivial features are only present in the correlation distance induced topology of the network showing a clear difference between the two operational modes. The healthy state features two cycles whereas the faulty one features only one, indicating the broken speed cycle.

logical invariant captures *which functional structure* changed and how robustly. This is precisely the level of description sought in a holistic PHM setting: not only that performance degraded, but that the organisation of control and feedback relationships changed with it.

7. DISCUSSION AND FUTURE WORK

The main point of this paper is conceptual as much as methodological: PHM for complex systems should not be limited to reading health from isolated channels. When degradation propagates through interaction pathways, the relevant health information is distributed across the structure of the system. The motor controller example supports this claim: edge density, mean edge strength, and persistent loop structure separate operating conditions in a way that is difficult to reproduce with a single-sensor view.

Our interconnectivity pipeline is one example of how such a relational PHM approach can be instantiated. It is not intended here as the final or exclusive solution. Other choices of interaction measure, representation, and topological summary may be better suited to other physical systems, and the ring stand-in case shows exactly why that flexibility matters: what one can detect depends on the relational measure one chooses.

Scaling to larger systems. The current validation cases involve a small number of channels with relatively clean coupling structure. Scaling to industrial systems with tens or hundreds of channels, non-stationary operating conditions, and overlapping failure modes is an open engineering challenge. Efficient topological approximations (landmark-based filtrations, witness complexes) will be required as channel count grows.

Directed graphs and causal structure. The example network used here is undirected: MI is symmetric and does not distinguish driver from driven. Transfer entropy and conditional MI can recover directed coupling, providing a basis for root-cause localisation in fault propagation chains. However, persistent homology and the Hodge Laplacian as developed here apply to undirected complexes; there is no established cohomology theory for directed graphs, and extending TDA to directed simplicial complexes is an active area of mathematical research.

Causal TDA. The longer-term goal is to combine causal learning — inferring the directed causal graph from observational or interventional data — with topological analysis performed on the resulting causal structure rather than the correlational proximity structure. This would allow fault-driven changes in causal pathways, not merely statistical coupling, to be captured as topological features, providing a more fundamental and interpretable basis for prognostics.

Interpretability and system structure. One reason topological summaries are attractive for PHM is that they reduce a large interaction object to a small number of interpretable structural descriptors. Betti numbers summarise connectedness and cyclic structure; Hodge-type spectral decompositions may help localise which components participate in those loops. Developing these summaries into actionable maintenance indicators remains an important next step.

REFERENCES

Battiston, F., Cencetti, G., Iacopini, I., Latora, V., Lucas, M., Patania, A., ... Petri, G. (2020, August). Networks beyond pairwise interactions: Structure and dynamics. *Physics Reports*, *874*, 1–92. doi: 10.1016/j.physrep.2020.05.004

Benjamini, Y., & Hochberg, Y. (2018, 12). Controlling the False Discovery Rate: a Practical and Powerful Approach to Multiple Testing. *Journal of the Royal Statistical Society: Series B (Methodological)*, *57*(1), 289-300.

Canolty, R. T., & Knight, R. T. (2010, November). The functional role of cross-frequency coupling. *Trends in Cognitive Sciences*, *14*(11), 506–515. doi: 10.1016/j.tics.2010.09.001

Frantzen, F., & Schaub, M. T. (2025). Hlsad: Hodge laplacian-based simplicial anomaly detection. In *Proceedings of the 31st acm sigkdd conference on knowledge discovery and data mining v. 2* (pp. 626–636).

Picinbono, B. (1997, March). On instantaneous amplitude and phase of signals. *IEEE Transactions on Signal Processing*, *45*(3), 552–560. doi: 10.1109/78.558469

Rosas, F., Mediano, P. A. M., Gastpar, M., & Jensen, H. J. (2019, September). Quantifying High-order Interdependencies via Multivariate Extensions of the Mutual Information. *Physical Review E*, *100*(3), 032305. (arXiv:1902.11239 [cs]) doi: 10.1103/PhysRevE.100.032305

Theiler, J., Eubank, S., Longtin, A., Galdrikian, B., Farmer, J. D., & Farmer, J. D. (1992). Testing for nonlinearity in time series: the method of surrogate data. *Physica D: Nonlinear Phenomena*, *58*(1), 77-94.

Torres, L., Blevins, A. S., Bassett, D., & Eliassi-Rad, T. (2021). The why, how, and when of representations for complex systems. *SIAM Review*, *63*(3), 435–485.

Tort, A. B. L., Komorowski, R., Eichenbaum, H., & Kopell, N. (2010, August). Measuring Phase-Amplitude Coupling Between Neuronal Oscillations of Different Frequencies. *Journal of Neurophysiology*, *104*(2), 1195–1210. doi: 10.1152/jn.00106.2010